Imaging Science in Dentistry 2024; 54: 362-9
https://doi.org/10.5624/isd.20240096

The influence of the field of view and voxel size on the contrast-to-noise ratio in cone-beam computed tomography imaging

Nezaket Ezgi Özer[1], Ali Canberk Ulusoy[1], Betul İlhan[1,*], Ninita Lindfors[2], Hayal Boyacıoğlu[3], Hans-Göran Gröndahl[2]

[1]*Department of Oral and Maxillofacial Radiology, School of Dentistry, Ege University, Bornova, Izmir, Turkiye*
[2]*Department of Oral and Maxillofacial Radiology, The Institute for Postgraduate Dental Education, Jönköping, Sweden*
[3]*Department of Statistics, Faculty of Science, Ege University, Izmir, Turkiye*

ABSTRACT

Purpose: This study investigated the impact of the field of view (FOV), voxel size, and exposure parameters on the contrast-to-noise ratio (CNR) in cone-beam computed tomography (CBCT).

Materials and Methods: A SedentexCT phantom was scanned using 3D Accuitomo 170 across 3 FOVs (40 × 40 mm, 60 × 60 mm, 80 × 80 mm). Each FOV had 4 settings for kVp and 3 for mA. Volumes were reconstructed with voxel sizes from 80 to 250 μm. The CNR was calculated using ImageJ (ver. 1.41, National Institutes of Health, Bethesda). Statistical analyses included Pearson correlation coefficients and regression (R^2).

Results: Positive correlations were observed in the 40 × 40 FOV between voxel size, kVp, mA, rotation degree, and CNR. The 60 × 60 FOV showed positive correlations between mA, kVp, and CNR, while the 80 × 80 FOV exhibited correlations for voxel size, kVp, and mA. In the 40 × 40 ($R^2 = 0.551$) and 80 × 80 ($R^2 = 0.550$) FOVs, mA, kVp, and voxel size influenced CNR. For the 60 × 60 FOV, mA and kVp were significant contributors ($R^2 = 0.389$). Using a constant 80-μm voxel size, both mA and kVp significantly influenced CNR ($R^2 = 0.467$); neither FOV nor rotation degree had substantial impacts.

Conclusion: CNR increased with higher mA, kVp, and larger voxel sizes for 40 × 40 and 80 × 80 FOVs. mA was the most influential factor across all FOVs. Regression models showed significant effects of mA and kVp on CNR with 80-μm voxels, while FOV had no effect. ***(Imaging Sci Dent 2024; 54: 362-9)***

KEY WORDS: Cone-Beam Computed Tomography, Tomography, Phantoms, Diagnostic Imaging, Signal-To-Noise Ratio

Introduction

Cone-beam computed tomography (CBCT) devices offer a wide range of exposure parameters, including tube voltage, tube current, exposure time, and rotation degree, as well as diverse field-of-views (FOVs) and voxel sizes. These factors collectively impact both radiation dose and image quality.[1,2] Differences in imaging performance can also arise from variations in detector types and reconstruction algorithms. Consequently, there is a need for systematic and quantitative analyses of image quality, with a focus on spatial resolution, contrast, and noise.[1,3,4] The influence of voxel size on image quality and spatial resolution is well-documented in the literature.[3-6] Contrast resolution, which is essential for distinguishing various contrast levels within an image, plays a significant role in CBCT scans.[7-10] In contrast, the contrast-to-noise ratio (CNR) assesses the balance between image contrast and noise, influencing the detectability of structures in tomographic images.[11,12] Higher CNR values are generally preferred as they indicate clearer differentiation between signal and background noise, corresponding to higher image quality that facilitates better visualization of structures and anomalies.[6-9] However, the optimal CNR varies depending on specific application needs and potential trade-offs. Several studies have explored CNR in

Received May 9, 2024; Revised July 3, 2024; Accepted August 23, 2024
Published online October 23, 2024
*Correspondence to : Prof. Betul İlhan
Department of Oral and Maxillofacial Radiology, School of Dentistry, Ege University, Bornova, Izmir, Turkiye
Tel) 90-532-343-42-76, E-mail) betul.ilhan@ege.edu.tr

CBCT imaging, focusing on the impact of different scanning parameters.[13-18] A positive influence of kVp on CNR has been reported in numerous studies.[19-22] Pauwels et al.[13] found that the highest kVp (specifically, 90 kVp) yielded the highest CNR at a consistent radiation dose, particularly at lower dose levels. Similarly, Ludlow and Walker[23] observed an increase in CNR with increasing kVp and mAs when voxel size and FOV were held constant. However, there is limited data on the effect of different FOVs and voxel sizes on CNR in CBCT images.[3,23-25] Niktash et al.[3] reported that CNR increased with larger FOVs in dry mandibles across various CBCT units. Conversely, Bechara et al.[25] and Ludlow and Walker[23] observed that CNR decreased with increasing FOV size in images from hemimaxilla embedded in resin and an anthropomorphic phantom, respectively. Comparing findings from previous studies is challenging due to variations in study materials across different investigations. The SedentexCT project developed a phantom that is universally applicable to all CBCT devices, aiming to standardize quantitative assessments of image quality in CBCT studies.[26] The phantom has already been used in several studies in which different aspects of image quality have been evaluated.[2,17,27,28] To achieve optimal image quality in different situations, it is crucial to carefully analyze all factors that may influence it. This is essential for making informed decisions about which settings to use. Therefore, the present study aimed to investigate the impact of FOV, voxel size, and exposure parameters on CNR in CBCT, through standardized assessments using the SedentexCT phantom.

Materials and Methods

Phantom and inserts

The SedentexCT IQ phantom (Leeds Test Objects Ltd., Boroughbridge, UK) was utilized to evaluate CNR. This cylindrical polymethyl methacrylate (PMMA) phantom, measuring 16 cm in diameter and 17.7 cm in height, simulates an adult head. It features a PMMA base, 1 central, and 6 surrounding cylindrical holes, each 34.5 mm in diameter and 20 mm in height, allowing the placement of different inserts for image quality analyses.[18] For CNR measurements, inserts measuring 3.5 cm in diameter and 2 cm in height were employed. These inserts included rods made of aluminum and 3 different densities of hydroxyapatite (HA) (50, 100, and 200 mg/cm^3) embedded in PMMA to represent both high- and low-contrast resolutions.

CBCT system

CBCT images were obtained using a 3D Accuitomo 170 (J. Morita, Kyoto, Japan), which features a focal spot size of 0.5 mm and inherent filtration of 3.1 mm Al at 70 kVp. The unit provides the operator with the ability to select exposure settings and offers 2 rotation protocols: 180° with a scan time of 9 seconds, and 360° with a scan time of 17.5 seconds. Approximately 300 and 560 images are acquired during the respective scans, each with a resolution of 512 × 512 matrices and a 13-bit grayscale depth.

Fig. 1. SedentexCT IQ phantom fixed with a custom-made apparatus.

The phantom was secured to the unit using a custom-made apparatus (Fig. 1), and a scout image was taken before the exposures. The phantom's position was marked in the axial, sagittal, and coronal directions to ensure consistent placement in future scanning sessions. Three different FOVs were employed: 40 × 40, 60 × 60, and 80 × 80 (mm diameter × mm height). For the 40 × 40 and 60 × 60 FOVs, the insert was positioned in the left column and middle level of the phantom, while for the 80 × 80 FOV, it was placed in the central column and middle level. The remaining columns were filled with homogeneous PMMA inserts. In summary, a total of 36 exposures were conducted for each FOV, utilizing varying mA (1 mA, 4 mA, and 8 mA), kVp (60-90 kVp), and voxel sizes to assess their impact on CNR. Additionally, 12 half scans (180°) were executed for each FOV using only the default voxel size and the same exposure parameters as mentioned earlier. Overall, 144 scans were completed (108 full scans and 36 half scans), with a selected slice

thickness and interval of 4 voxels for each scan.

After each exposure, images were retrieved using i-Dixel 2.0 software (J. Morita, Kyoto, Japan). A central axial slice image for each material within the insert was then selected and exported as a DICOM file using the same software. These images were saved on a personal computer for further analysis.

Calculation of CNR

For each material, the mean gray value (MGV) and standard deviation (SD) were measured using ImageJ (ver. 1.41, National Institutes of Health, Bethesda, MD). PMMA served as the background material. Circular regions of interest (ROIs) were placed on the inner part of each material and on the PMMA. To account for variations in image size, a specific ROI was established for each FOV and voxel size. This ROI was consistently reproduced for each FOV and voxel size to maintain consistency in ROI positioning. The CNR for each material was calculated by subtracting the background MGV (PMMA) from the material MGV and

Table 1. Contrast-to-noise (CNR) values for each material and scan for 360° and default voxel sizes

Field of view	Voxel size	kVp	mA	CNR-HA50	CNR-HA100	CNR-HA200	CNR-Aluminum
4 cm × 4 cm	80 μm (default size)	60	1	0.23	0.25	0.99	2.00
		60	4	0.65	0.59	2.42	4.18
		60	8	0.93	0.84	3.60	5.98
		70	1	0.42	0.36	1.42	2.90
		70	4	0.86	0.75	3.27	6.27
		70	8	1.09	1.10	4.44	8.68
		80	1	0.50	0.48	1.89	3.70
		80	4	0.96	0.90	3.83	8.03
		80	8	1.20	1.16	4.99	10.43
		90	1	0.60	0.57	2.23	4.52
		90	4	1.05	1.00	4.23	9.07
		90	8	1.23	1.25	5.36	11.40
6 cm × 6 cm	125 μm (default size)	60	1	0.48	0.40	1.73	3.20
		60	4	1.22	1.07	4.34	6.83
		60	8	1.74	1.57	6.40	9.41
		70	1	0.76	0.65	2.48	4.81
		70	4	1.51	1.53	5.83	9.83
		70	8	2.02	2.26	8.31	12.60
		80	1	0.95	0.87	3.40	6.30
		80	4	1.82	1.70	6.97	12.36
		80	8	2.52	2.67	9.88	15.54
		90	1	1.07	1.05	3.98	7.56
		90	4	2.04	2.00	7.99	13.85
		90	8	2.81	2.76	11.28	17.77
8 cm × 8 cm	160 μm (default size)	60	1	0.55	0.56	1.73	3.03
		60	4	1.36	1.23	4.42	6.96
		60	8	1.90	1.74	6.57	10.56
		70	1	0.75	0.77	2.50	4.37
		70	4	1.59	1.67	5.67	9.95
		70	8	2.44	2.21	7.98	13.94
		80	1	0.98	0.92	3.39	5.95
		80	4	2.06	1.97	6.77	13.10
		80	8	3.01	2.63	9.55	17.49
		90	1	1.20	1.26	4.17	8.18
		90	4	2.42	2.34	8.83	16.03
		90	8	3.31	3.42	11.59	20.68

dividing the result by the mean of their SDs.

$$CNR = (MGV_{PMMA} - MGV_{Material}) / SD_{PMMA, Material}$$

The absolute value was used to prevent negative values for materials other than aluminum. Statistical analysis was conducted using IBM SPSS Statistics for Windows ver. 25.0 (IBM Corp, Armonk, USA). The Pearson correlation test was applied to assess the relationship, including its degree and direction, between CNR and other variables across various FOVs and voxel sizes. Following this, regression analysis was performed, and coefficients of determination (R^2) were calculated to evaluate the impact of scan parameters on CNR. The significance level was set at $P<0.05$.

Results

Table 1 presents CNR values for each material and scan protocol. Due to large amount of data, only CNR values for 360° scans and default voxel sizes are shown. When analyzing each FOV separately, a positive correlation was found between voxel size (r=0.402, $P<0.05$), kVp (r=0.234, $P<0.05$), mA (r=0.292, $P<0.05$), rotation degree (r=0.252, $P<0.05$), and CNR for the 40×40 FOV. This indicates that increases in voxel size, mA, kVp, and rotation degree lead to higher CNR values for all materials. In the 60×60 FOV, positive correlations were observed between mA (r=0.343, $P<0.05$) and kVp (r=0.176, $P<0.05$) and CNR. For the 80×80 FOV, voxel size (r=0.252, $P<0.05$), kVp (r=0.254, $P<0.05$), and mA (r=0.395, $P<0.05$) showed positive correlations (Table 2). Regression analysis indicated that for the 40×40 and 80×80 FOVs, the most significant parameters affecting CNR were mA, kVp, and voxel size (all $P<0.05$), with R^2 values of 0.551 and 0.550, respectively, demonstrating strong explanatory power. For the 60×60 FOV, mA and kVp were significant factors, with an R^2 of 0.389, indicating that the model had moderate explanatory capability.

Table 2. The influence of different exposure parameters on the contrast-to-noise ratio (CNR) for each field of view for all materials

	4 cm×4 cm		6 cm×6 cm		8 cm×8 cm	
	r	*P*	r	*P*	r	*P*
Voxel size	.402	<0.05	.034	.639	.252	<0.05
kVp	.234	<0.05	.176	<0.05	.254	<0.05
mA	.292	<0.05	.343	<0.05	.395	<0.05
Rotation	.252	<0.05	.044	.542	.100	.168

r: Pearson correlation coefficient

Each FOV offered different voxel size options, but 80 μm was the only size consistently available across all FOVs. The correlation analysis using this voxel size indicated a positive correlation between mA (r=0.383, $P<0.05$) and kVp (r=0.233, $P<0.05$) and CNR. When the voxel size was held constant at 80 μm, neither the FOV nor the degree of rotation significantly affected CNR. Additionally, voxel sizes of 125 μm (60×60, r=0.396, $P<0.05$), 160 μm

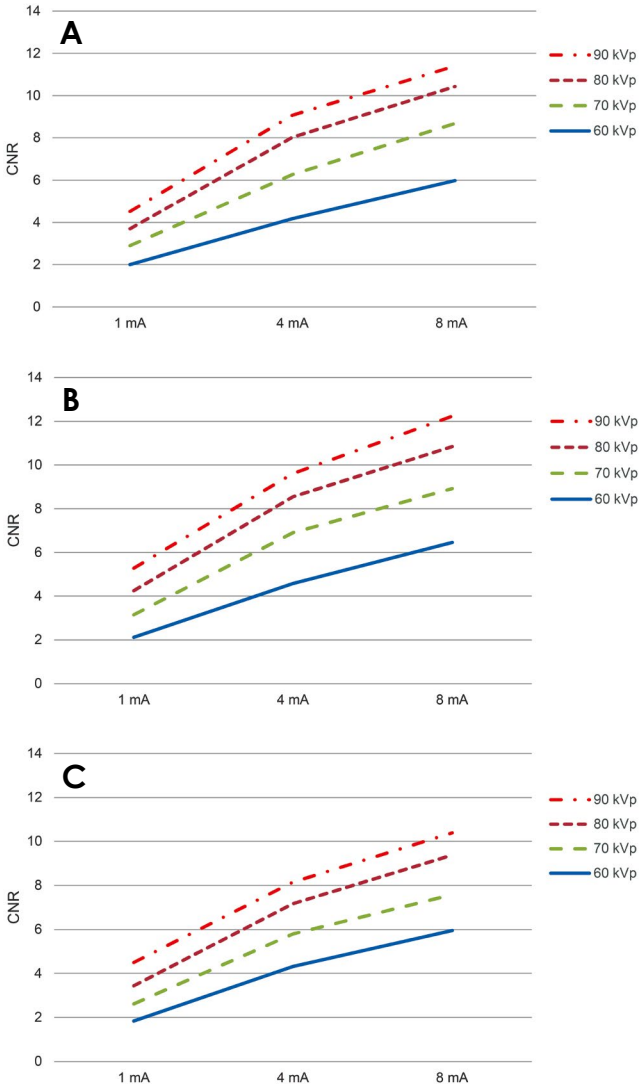

Fig. 2. Using a constant 80-μm t voxel size (A, B, C), both mA and kVp significantly influenced the contrast-to-noise ratio (CNR) (R^2=0.467), while neither field of view (FOV) nor rotation degree had substantial impacts. A. Variations in CNR values for aluminum at different mA and kVp settings using a 40×40 FOV, 80 μm voxel size, and 360° rotation. B. Variations in CNR values for aluminum at different mA and kVp settings using a 60×60 FOV, 80 μm voxel size, and 360° rotation. C. Variations in CNR values for aluminum at different mA and kVp settings using an 80×80 FOV, 80 μm voxel size, and 360° rotation.

(40×40, 80×80, $r = 0.394$, $P < 0.05$), 200 μm (60×60, 80×80, $r = 0.324$, $P < 0.05$), and 250 μm (40×40, $r = 0.315$, $P < 0.05$) all showed positive correlations with CNR. Regression analysis revealed that at a constant voxel size of 80 μm, both mA ($P < 0.05$) and kVp ($P < 0.05$) significantly influenced CNR, demonstrating a strong relationship with an R^2 of 0.467 (Fig. 2).

Discussion

Like any imaging technology, CBCT has recognized limitations, including the potential for an increased radiation dose, the generation of artifacts, scatter, noise, and variations in dose distribution within a volume of interest that can impact image quality.[19] The acquisition settings—tube voltage, tube current, exposure time, rotation degree, FOV, and voxel size—play a critical role in shaping image quality,[29] and maintaining diagnostically acceptable images requires meticulous adjustments in response to alterations in any of these parameters. CNR is a widely employed metric for image quality assessment factor that is associated with quality rather than noise. It is one of many factors that depend on achieving an acceptable level of lesion-to-background contrast.[24] As a standard factor in image quality evaluation, CNR has been extensively studied in various applications, including the optimization of device settings.[3,12,17,26,29] However, the effects of FOV and voxel size on CNR have been rarely evaluated in previous studies,[3,23-25] and instead have often been mentioned incidentally as a secondary observation. Hence, in order to perform an objective evaluation, this study employed CNR as a technical parameter to assess image quality, using a SedentexCT phantom to ensure standardized quantitative assessments. Additionally, all the available FOVs in 3D Accuitomo 80 were used with commonly utilized voxel sizes and exposure protocols.

Based on regression analysis of all materials, this study found that for a given FOV, CNR tended to increase with higher mA and kVp. Additionally, for FOVs measuring 40×40 mm and 80×80 mm, CNR also increased with larger voxel sizes. Regression models indicated that mA was the most significant factor affecting CNR across all FOVs. In this study, the only consistent voxel size used across all 3 FOVs was 80 μm. The regression model demonstrated that both mA and kVp significantly influenced CNR when images were reconstructed using this voxel size, whereas the FOV did not have a significant impact. These findings are consistent with some previous studies but differ from others. However, it is important to note that direct comparisons between studies can be problematic due to variations in study materials, exposure parameters, and CBCT units. The present study highlights this limitation, as it was conducted using only 1 specific CBCT device and a single image quality phantom.

Using dry mandibles, Niktash et al.[3] explored the impact of different FOV sizes on CNR across various CBCT units. They reported that, despite the type of imaging modality and varying exposure parameters in each CBCT unit, CNR increased with larger FOVs. However, significant differences in CNR were noted when comparing similar FOVs across different units. Conversely, Bechara et al., using 3 large FOVs (20×19 cm, 16×10 cm, 16×7 cm), found that CNR decreases with increasing volume size in images from hemimaxilla embedded in resin,[25] and Ludlow and Walker[23] observed a modest reduction in CNR in images from an anthropomorphic phantom as the diameter of the FOV increased. Unlike these previous reports, in the authors' prior study with a constant voxel size, FOV size had no impact on CNR. It has been reported that a larger FOV increases both the magnitude of generated scatter (due to the increased total number of X-ray photons) and the proportion of detected scatter (due to the larger active detector area), which in turn results in decreased contrast resolution and increased noise,[30,31] and therefore improved image quality can be expected in smaller FOVs.[31,32] The selection of FOV size and positioning is dictated by the specific diagnostic region of interest. The decrease in image quality observed in larger FOVs, attributed to scatter, has been acknowledged as an additional incentive to minimize the FOV size whenever practical.[30] Consistent with earlier studies, the results of the present study indicate that the larger FOVs do not necessarily lead to an improvement in image quality, in terms of CNR. Hence, it is recommended to restrict the FOV selection to the specific area of interest, reserving the use of larger volumes solely for scenarios necessitating a comprehensive view of diverse dentofacial structures.

In an individual assessment of each FOV, the regression analysis revealed a favorable impact of voxel size on CNR for volume sizes of 40×40 mm and 80×80 mm, whereas such an influence was not observed for the 60×60 mm FOV. Although positive correlations between voxel size and CNR were noted within the 60×60 mm FOV, which utilized voxel sizes of 80 μm, 125 μm, and 200 μm, regression analysis did not identify voxel size as a significant factor influencing CNR, unlike in the 40×40 mm and 80×80 mm FOVs. This discrepancy may be attributed to the specific reconstruction algorithms applied to different voxel sizes, as well as the local tomography effect observed in smaller FOVs, where only part of the object is included, affecting

the calculations.[3] Nonetheless, since each FOV featured different voxel size options, focusing on the common 80 μm voxel size enhanced the accuracy and comparability of the analysis, ensuring consistent results across the various FOVs in this study.

Tanimoto and Arai[8] examined the effects of 3 different voxel sizes (40, 80, and 160 μm) on the resolution and noise in CBCT images, and reported that smaller voxel sizes were associated with increased noise, and identified 80 μm as the resolution limit. While a smaller voxel size can enhance spatial resolution, achieving this in the context of a specific flat panel detector, considering pixel fill factor, may require a higher radiation dose.[32] Reduced X-ray photon detection is observed with smaller voxel sizes than with larger voxel sizes, and this has been documented to result in diminished signal and increased noise levels.[8,24,33] In accordance with previous reports, the present findings indicate that a smaller voxel size does not necessarily lead to an increase in CNR,[3,8,33,34] and for a given FOV, CNR increases with increasing voxel size.[23,24]

The impact of tube voltage and tube current on contrast, noise, and scatter radiation in CBCT involves a complex interplay, particularly with regard to noise.[35] Noise is linearly related to mA, whereas the relationship between kVp and image noise is more complex. This complexity arises because kVp influences photon production in the X-ray tube through radiative stopping power, causing noise levels to vary as a function of kVp.[25] A higher kVp increases the signal at the X-ray detector by increasing the photon energy, which increases the X-ray penetration; therefore, the percentage of the X-ray intensity incident on the patient that is transmitted also increases.[30,36] Thus, increasing the kVp will reduce the amount of noise observed in the resultant images. It is also important to note that a high kVp generates a larger percentage of scatter radiation, which reduces radiographic contrast by overlaying additional gray noise on the image signal captured by the image receptor.[30] As in previous observations, a positive influence of kVp on CNR was noted in the present study.[19-22] Similarly, investigating the optimal kVp in CBCT, Pauwels et al.[13] concluded that the highest kVp (specifically, 90 kVp), yielded the highest CNR at a consistent radiation dose, and this tendency was particularly evident at lower dose levels. However, the regression models in the present study identified mA as the most influential parameter on CNR across all FOVs. An increase in mA, or dose, leads to greater electron production and consequently, an increase in x-radiation. This results in more photons reaching the detector, thereby reducing apparent structural density. While increasing mA does not affect contrast, it does reduce image noise by increasing the signal at the detector.[13] Similar to these findings, Ludlow and Walker[23] reported that when voxel size and FOV were held constant, an increase in CNR was seen with increasing energy and mAs. Additionally, Klintström et al.[37] showed an increase in CNR with increasing dose, and they reported that increasing the tube current from 5 to 8 mA resulted in a significant increase in CNR. Elkhateeb et al.[20] substantiated these findings, noting that with consistent FOV and voxel size, the low-dose protocols resulted in considerably lower CNR values. In contrast to the observations in the present study, which demonstrated a favorable impact of mA on CNR across all voxel sizes, Klintström et al.[37] observed this increase solely with a 125-μm voxel size.

The current investigation also assessed the impact of 2 rotation modes on CNR (180° with a scan time of 9 s and 360° with a scan time of 17.5 s) with the 3D Accuitomo. Using small FOVs, Bechara et al. reported that the Accuitomo 360° scan outperformed the Accuitomo 180° scan in terms of CNR.[24] Similarly, the findings of this study indicate an increase in CNR with the 360° scan over the 180° scan, especially noticeable in the 40 × 40 mm FOV. This improvement is likely due to the doubling of basis images obtained. Interestingly, for larger FOVs (60 × 60 mm, 80 × 80 mm), the rotation had no significant effect on CNR, consistent with previous research.[3,24,25] Therefore, these results support the use of shorter scan times for larger FOVs, a method that reduces patient radiation exposure without sacrificing image quality in this particular CBCT unit.

Optimal imaging technology should aim to produce images characterized by superior quality, which means achieving efficient CNR and clear soft-tissue differentiation. The impact of altering exposure settings on both image quality and dose is complex, requiring a careful balance to achieve acceptable image quality at the lowest feasible dose level. Evaluating technical image quality, such as CNR, offers an objective method to examine this delicate balance. While this study provides valuable insights into the technical parameters that influence CNR in CBCT, it is crucial to recognize its limitations. In a clinical setting, numerous factors beyond exposure settings affect image quality, including patient size, motion, and artifacts such as beam hardening and the exponential edge-gradient effect. Establishing reference levels for CNR in CBCT is challenging due to the complex nature of diagnostic image quality, which depends not only on contrast and noise but also on spatial resolution. Moreover, the lack of well-established objective criteria for evaluating the diagnostic quality of CBCT images further complicates this task. Another limitation in using technical image quality

parameters for assessment is the absence of a direct method to translate these parameters into clinical image quality, as highlighted by Wang et al.[29] Therefore, despite the clarity provided by technical metrics like CNR, distinguishing between clinically acceptable and unacceptable values remains an ongoing challenge in CBCT image evaluation.[13]

The present study investigated the relationship between acquisition settings and image quality in terms of CNR in CBCT imaging. It was found that for a given FOV, CNR displayed an increasing trend with higher mA and kVp. Furthermore, when focusing on FOVs of 40 × 40 mm and 80 × 80, CNR exhibited an additional rise with increasing voxel size. The analysis revealed that mA is the most influential parameter affecting CNR across all FOVs, as demonstrated by the regression models. These models also showed that both mA and kVp significantly impact CNR when reconstructing images from all volumes with an 80 μm voxel size, whereas FOV showed no significant effect. Moreover, an increase in CNR was noted with a 360° scan compared to a 180° scan for the smallest FOV, suggesting that shorter scanning times might be viable for larger FOVs.

Conflicts of Interest: None

References

1. Scarfe WC, Li Z, Aboelmaaty W, Scott SA, Farman AG. Maxillofacial cone beam computed tomography: essence, elements and steps to interpretation. Aust Dent J 2012; 57 Suppl 1: 46-60.
2. Bamba J, Araki K, Endo A, Okano T. Image quality assessment of three cone beam CT machines using the SEDENTEXCT CT phantom. Dentomaxillofac Radiol 2013; 42: 20120445.
3. Niktash A, Mehralizadeh S, Talaeipour A. The effect of different field of view sizes on contrast-to-noise ratio of cone-beam computed tomography units: an in-vitro study. Front Dent 2022; 19: 32.
4. Khurana S, Parasher P, Creanga AG, Geha H. Effect of mandible phantom inclination in the axial plane on image quality in the presence of implant using cone-beam computer tomography. Cureus 2023; 15: e36630.
5. Wood R, Sun Z, Chaudhry J, Tee BC, Kim DG, Leblebicioglu B, et al. Factors affecting the accuracy of buccal alveolar bone height measurements from cone-beam computed tomography images. Am J Orthod Dentofacial Orthop 2013; 143: 353-63.
6. Damstra J, Fourie Z, Huddleston Slater JJ, Ren Y. Accuracy of linear measurements from cone-beam computed tomography-derived surface models of different voxel sizes. Am J Orthod Dentofacial Orthop 2010; 137: 16.e1-6.
7. Park HJ, Jung SE, Lee YJ, Cho WI, Do KH, Kim SH, et al. The relationship between subjective and objective parameters in CT phantom image evaluation. Korean J Radiol 2009; 10: 490-5.
8. Tanimoto H, Arai Y. The effect of voxel size on image reconstruction in cone-beam computed tomography. Oral Radiol 2009; 25: 149-53.
9. Siewerdsen JH, Jaffray DA. Cone-beam computed tomography with a flat-panel imager: magnitude and effects of x-ray scatter. Med Phys 2001; 28: 220-31.
10. Rohani SA, Ghomashchi S, Umoh J, Holdsworth DW, Agrawal SK, Ladak HM. Iodine potassium iodide improves the contrast-to-noise ratio of micro-computed tomography images of the human middle ear. J Microsc 2016; 264: 334-8.
11. Li X, Huang W, Rooney WD. Signal-to-noise ratio, contrast-to-noise ratio and pharmacokinetic modeling considerations in dynamic contrast-enhanced magnetic resonance imaging. Magn Reson Imaging 2012; 30: 1313-22.
12. Lindfors N, Lund H, Johansson H, Ekestubbe A. Influence of patient position and other inherent factors on image quality in two different cone beam computed tomography (CBCT) devices. Eur J Radiol Open 2017; 4: 132-7.
13. Pauwels R, Silkosessak O, Jacobs R, Bogaerts R, Bosmans H, Panmekiate S. A pragmatic approach to determine the optimal kVp in cone beam CT: balancing contrast-to-noise ratio and radiation dose. Dentomaxillofac Radiol 2014; 43: 20140059.
14. Elstrøm UV, Muren LP, Petersen JB, Grau C. Evaluation of image quality for different kV cone-beam CT acquisition and reconstruction methods in the head and neck region. Acta Oncol 2011; 50: 908-17.
15. Loubele M, Jacobs R, Maes F, Denis K, White S, Coudyzer W, et al. Image quality vs radiation dose of four cone beam computed tomography scanners. Dentomaxillofac Radiol 2008; 37: 309-18.
16. Suomalainen A, Kiljunen T, Käser Y, Peltola J, Kortesniemi M. Dosimetry and image quality of four dental cone beam computed tomography scanners compared with multislice computed tomography scanners. Dentomaxillofac Radiol 2009; 38: 367-78.
17. Choi JW, Lee SS, Choi SC, Heo MS, Huh KH, Yi WJ, et al. Relationship between physical factors and subjective image quality of cone-beam computed tomography images according to diagnostic task. Oral Surg Oral Med Oral Pathol Oral Radiol 2015; 119: 357-65.
18. Peltonen LI, Aarnisalo AA, Kortesniemi MK, Suomalainen A, Jero J, Robinson S. Limited cone-beam computed tomography imaging of the middle ear: a comparison with multislice helical computed tomography. Acta Radiol 2007; 48: 207-12.
19. Demirturk Kocasarac H, Helvacioglu Yigit D, Bechara B, Sinanoglu A, Noujeim M. Contrast-to-noise ratio with different settings in a CBCT machine in presence of different root-end filling materials: an in vitro study. Dentomaxillofac Radiol 2016; 45: 20160012.
20. Elkhateeb SM, Torgersen GR, Arnout EA. Image quality assessment of clinically-applied CBCT protocols using a QAT phantom. Dentomaxillofac Radiol 2016; 45: 20160075.
21. Bechara BB, Moore WS, McMahan CA, Noujeim M. Metal artefact reduction with cone beam CT: an in vitro study. Dentomaxillofac Radiol 2012; 41: 248-53.
22. Kim S, Yoo S, Yin FF, Samei E, Yoshizumi T. Kilovoltage cone-beam CT: comparative dose and image quality evaluations in partial and full-angle scan protocols. Med Phys 2010; 37: 3648-59.
23. Ludlow JB, Walker C. Assessment of phantom dosimetry and image quality of i-CAT FLX cone-beam computed tomography.

Am J Orthod Dentofacial Orthop 2013; 144: 802-17.
24. Bechara B, McMahan CA, Moore WS, Noujeim M, Geha H, Teixeira FB. Contrast-to-noise ratio difference in small field of view cone beam computed tomography machines. J Oral Sci 2012; 54: 227-32.
25. Bechara B, McMahan CA, Moore WS, Noujeim M, Geha H. Contrast-to-noise ratio with different large volumes in a cone-beam computerized tomography machine: an in vitro study. Oral Surg Oral Med Oral Pathol Oral Radiol 2012; 114: 658-65.
26. Pauwels R, Stamatakis H, Manousaridis G, Walker A, Michielsen K, Bosmans H, et al. Development and applicability of a quality control phantom for dental cone-beam CT. J Appl Clin Med Phys 2011; 12: 3478.
27. Pauwels R, Beinsberger J, Stamatakis H, Tsiklakis K, Walker A, Bosmans H, et al. Comparison of spatial and contrast resolution for cone-beam computed tomography scanners. Oral Surg Oral Med Oral Pathol Oral Radiol 2012; 114: 127-35.
28. Pauwels R, Stamatakis H, Bosmans H, Bogaerts R, Jacobs R, Horner K, et al. Quantification of metal artifacts on cone beam computed tomography images. Clin Oral Implants Res 2013; 24 Suppl A100: 94-9.
29. Wang MF, Xie X, Li G, Zhang Z. Relationship between CNR and visibility of anatomical structures of cone-beam computed tomography images under different exposure parameters. Dentomaxillofac Radiol 2020; 49: 20190336.
30. Pauwels R, Pittayapat P, Sinpitaksakul P, Panmekiate S. Scatter-to-primary ratio in dentomaxillofacial cone-beam CT: effect of field of view and beam energy. Dentomaxillofac Radiol 2021; 50: 20200597.
31. Schulze R, Heil U, Gross D, Bruellmann DD, Dranischnikow E, Schwanecke U, et al. Artefacts in CBCT: a review. Dentomaxillofac Radiol 2011; 40: 265-73.
32. White SC, Pharaoh MJ. Oral radiology: principles and interpretation. 6th ed. St. Louis: Mosby/Elsevier; 2009. p. 131.
33. Maloul A, Fialkov J, Whyne C. The impact of voxel size-based inaccuracies on the mechanical behavior of thin bone structures. Ann Biomed Eng 2011; 39: 1092-100.
34. Kursun-Cakmak EŞ, Demirturk Kocasarac H, Bayrak S, Ustaoğlu G, Noujeim M. Estimation of contrast-to-noise ratio in CT and CBCT images with varying scan settings in presence of different implant materials. Dentomaxillofac Radiol 2019; 48: 20190139.
35. Brooks RA, Di Chiro G. Statistical limitations in x-ray reconstructive tomography. Med Phys 1976; 3: 237-40.
36. Pauwels R, Seynaeve L, Henriques JC, de Oliveira-Santos C, Souza PC, Westphalen FH, et al. Optimization of dental CBCT exposures through mAs reduction. Dentomaxillofac Radiol 2015; 44: 20150108.
37. Klintström E, Smedby O, Klintström B, Brismar TB, Moreno R. Trabecular bone histomorphometric measurements and contrast-to-noise ratio in CBCT. Dentomaxillofac Radiol 2014; 43: 20140196.